Comparative Functioning of Dihydro- and Tetrahydropterins in Supporting Electron Transfer, Catalysis, and Subunit Dimerization in Inducible Nitric Oxide Synthase†

Anthony Presta,‡ Uma Siddhanta,‡ Chaoqun Wu,‡ Nicolas Sennequier,‡ Liuxin Huang,‡ Husam M. Abu-Soud,‡ Serpil Erzurum,§ and Dennis J. Stuehr*,‡

Departments of Immunology and Cancer Biology, The Cleveland Clinic Foundation Lerner Research Institute, Cleveland, Ohio 44195

Received August 6, 1997; Revised Manuscript Received October 16, 1997⊗

ABSTRACT: The nitric oxide synthases (NOS) are the only heme-containing enzymes that require tetrahydrobiopterin (BH4) as a cofactor. Previous studies indicate that only the fully reduced (i.e., tetrahydro) form of BH4 can support NO synthesis. Here, we characterize pterin-free inducible NOS (iNOS) and iNOS reconstituted with eight different tetrahydro- or dihydropterins to elucidate how changes in pterin side-chain structure and ring oxidation state regulate iNOS. Seven different enzyme properties that are important for catalysis and are thought to involve pterin were studied. Only two properties were found to depend on pterin oxidation state (i.e., they required fully reduced tetrahydropterins) and were independent of side chain structure: NO synthesis and the ability to increase heme-dependent NADPH oxidation in response to substrates. In contrast, five properties were exclusively dependent on pterin side-chain structure or stereochemistry and were independent of pterin oxidation state: pterin binding affinity, and its ability to shift the heme iron to its high-spin state, stabilize the ferrous heme iron coordination structure, support heme iron reduction, and promote iNOS subunit assembly into a dimer. These results clarify how structural versus redox properties of the pterin impact on its multifaceted role in iNOS function. In addition, the data reveal that during NO synthesis all pterin-dependent steps up to and including heme iron reduction can take place independent of the pterin ring oxidation state, indicating that the requirement for fully reduced pterin occurs at a point in catalysis beyond heme iron reduction.

Nitric oxide (NO)[1] has emerged as a significant signaling and effector molecule in many physiologic systems, including the immune, cardiovascular, and nervous systems (for reviews see refs *1*−*3*). To fulfill its diverse functions, NO is generated *in vivo* by a family of three similar yet distinct enzymes collectively termed the NO synthases (NOS). Two of these, endothelial NOS and neuronal NOS, are constitutively expressed (*4*), whereas a third inducible isoform (iNOS) is expressed only in cells exposed to endotoxins or inflammatory cytokines (*5*−*7*).

The three NOS exhibit a similar catalytic profile and composition. They each catalyze an NADPH- and O_2-dependent five-electron oxidation of L-arginine to generate L-citrulline and NO, via formation of N^{ω}-hydroxy-L-arginine (NOHA) as an intermediate (*8*−*12*). All NOS are homodimers, with each subunit composed of two functional domains. The carboxy-terminal domain contains binding sites for NADPH, FAD, and FMN (*5*) and bears much resemblance to the cytochrome P-450 reductases; hence this domain of NOS is called the reductase domain. The reductase domain also contains a binding site for calmodulin, which reversibly binds to the constitutive NOS isoforms depending on the Ca^{2+} concentration but irreversibly binds to iNOS independent of the Ca^{2+} concentration (*13*). The amino-terminal half of each NOS isoform is an oxygenase domain that binds Fe-protoporphyrin IX (heme), L-arginine, and (6*R*)-tetrahydrobiopterin [(6*R*)-BH4] (*14*−*17*). The NOS oxygenase domains contain a cysteine thiolate that directly coordinates to the heme iron as an axial ligand (*18*−*22*). Substrate binding occurs in the vicinity of the heme, causing alterations in the electronic field around the ferric iron and a Type 1 shift in the UV−visible spectrum from low-spin to high-spin iron(III) (*23*−*26*). In the presence of bound calmodulin, the heme iron can accept NADPH-derived electrons from the reductase domain flavins (*27*). When

† This work was supported by National Institutes of Health Grant CA53914 to D.J.S. D.J.S. is an Established Investigator of the American Heart Association. A.P. is a Harriet B. Lawrence Fellow of the American Heart Association, Northeastern Ohio Affiliate.

* To whom correspondence should be addressed at Immunology, NN1, The Cleveland Clinic, 9500 Euclid Ave., Cleveland, OH 44195. Telephone (216) 445 6950; Fax (216) 444 9329; E-mail stuehrd@cesmtp.ccf.org.

‡ Department of Immunology.

§ Department of Cancer Biology.

⊗ Abstract published in *Advance ACS Abstracts,* December 15, 1997.

[1] Abbreviations: NO, nitric oxide; NOS, nitric oxide synthase; iNOS, macrophage inducible nitric oxide synthase; NADPH, nicotinamide adenine dinucleotide phosphate (reduced); FAD, flavin adenine dinucleotide; FMN, flavin mononucleotide; (6*R*)-BH4, (6*R*)-tetrahydrobiopterin, (6*R*)-5,6,7,8-tetrahydro-L-biopterin; BH2, 7,8-dihydro-L-biopterin; NH4, (6*R*,*S*)-5,6,7,8-tetrahydro-D-neopterin; 6-OHMePH4, (6*R*,*S*)-6-hydroxymethyl-5,6,7,8-tetrahydropterin; 6-MePH4, (6*R*,*S*)-6-methyl-5,6,7,8-tetrahydropterin; NOHA, N^{ω}-hydroxy-L-arginine; NMA, N^{ω}-methyl-L-arginine; AGPA, L-α-amino-β-guanidinopropionic acid; thiocitrulline, *d*-(thioureido)-L-norvaline; EPPS, 4-(2-hydroxyethyl)-1-piperazinepropanesulfonic acid; HEPES, 4-(2-hydroxyethyl)-1-piperazineethanesulfonic acid; DTT, dithiothreitol; BSA, bovine serum albumin; SOD, superoxide dismutase; IPTG, isopropyl β-D-thiogalactopyranoside; PMSF, phenylmethanesulfonyl fluoride; NTA, nitrilotriacetate; CO, carbon monoxide; HPLC, high-pressure liquid chromatography.

S0006-2960(97)01944-2 CCC: $15.00
Published on Web 01/06/1998

reduced, the ferrous heme can bind O_2 (*28*, *29*) and then proceed with the oxygenation of substrate.

The NOSs are the only heme-containing enzymes known to require a pterin cofactor for activity. BH4 appears to support NO synthesis only in its fully reduced (i.e., tetrahydro) form (*30*−*33*); however, the basis for this requirement is unclear. Most studies of BH4 function have been limited by an unavailability of pterin-free NOS preparations. Nevertheless, a number of functions have been proposed including stabilization of the NOS active dimeric structure (*19*, *34*−*38*), promotion of subunit dimerization for iNOS (*35*, *39*, *40*), allosteric modulation of the enzyme (*33*, *34*, *38*, *41*), and attenuation of the feedback inhibition by NO (*42*, *43*). A possible role for BH4 in providing electron equivalents for heme reduction and/or oxygen activation had also been proposed (*30*, *31*, *44*) on the basis of its known function in aromatic amino acid hydroxylation (*45*). However, it was subsequently shown that NOS utilize an NADPH- and flavin-based reductase system to provide reducing equivalents to its heme, much unlike the aromatic amino acid hydroxylases that utilize BH4 as a sole source of electrons. Moreover, mechanistic considerations indicate that NOS is supplied with sufficient reducing equivalents by NADPH and substrate to fully account for NO synthesis (*1*, *11*, *12*, *46*), implying that no additional electrons are needed from BH4. Consistent with this, redox cycling of the pterin cofactor has not been detected during catalysis by NOS (*34*, *47*), although experimental difficulties may limit investigation of BH4 redox cycling in NOS. Thus, results to date suggest that (6*R*)-BH4 supports NO synthesis by a variety of means that do not neccessarily involve its redox cycling.

To better define BH4's role in regulating NOS structure and catalysis, we have characterized a pterin-free form of mouse iNOS expressed in *Escherichia coli* reconstituted with a number of tetrahydro- and dihydropterins, alone or in conjunction with L-arginine or substrate analogues. Each pterin's capacity to affect the electronic, catalytic, and structural properties of iNOS is compared and discussed with regard to (6*R*)-BH4 function in NO synthesis.

MATERIALS AND METHODS

Materials. The pterin analogues used in this study are shown in Figure 1, along with their structural formulas and designations. All pterin analogues were purchased from Dr. B. Schirck's laboratory (Jona, Switzerland). The tetrahydropterin analogues were dissolved in 40 mM 4-(2-hydroxyethyl)-1-piperazinepropanesulfonic acid (EPPS) buffer, pH 7.6, with a 3-fold molar excess of dithiothreitol (DTT). The dihydropterins were dissolved in dimethyl sulfoxide. All pterin solutions were kept at −70 °C when not in use. Agmatine, L-α-amino-β-guanidinopropionic acid (AGPA), *N*-aminoguanidine, δ-aminolevulinic acid, ammonium sulfate, L-arginine, bovine serum albumin (BSA), chloramphenicol, L-citrulline, EPPS, 4-(2-hydroxyethyl)-1-piperazineethanesulfonic acid (HEPES), homoarginine, imidazole, sodium dithionite, sodium nitrate, sodium nitrite, and superoxide dismutase were purchased from Sigma (St. Louis, MO). Ampicillin, catalase, FAD, FMN and isopropyl β-D-thiogalactopyranoside (IPTG) were purchased from Boehringer Mannheim GmbH (Germany). NOHA and N^{ω}-methyl-L-arginine (NMA) were purchased from Alexis (San Diego, CA). DTT and *S*-ethylisothiourea (SEITU) were purchased from Aldrich (Milwaukee, WI). *N*-Hydroxyguanidine was purchased from Pfaltz and Bauer (Waterbury, CT). Urea was purchased from Bio-Rad (Richmond, CA). Glycerol and Terrific Broth were purchased from Gibco-BRL Life Technologies (Gaithersburg, MD). His-Bind (nitrilotriacetate, NTA) resin was purchased from Novagen (Madison, WI). Carbon monoxide was purchased from Gas Technics (Cleveland, OH). L-Thiocitrulline was a gift from Dr. P. L. Feldman, Glaxo Research Institute, Research Triangle Park, NC.

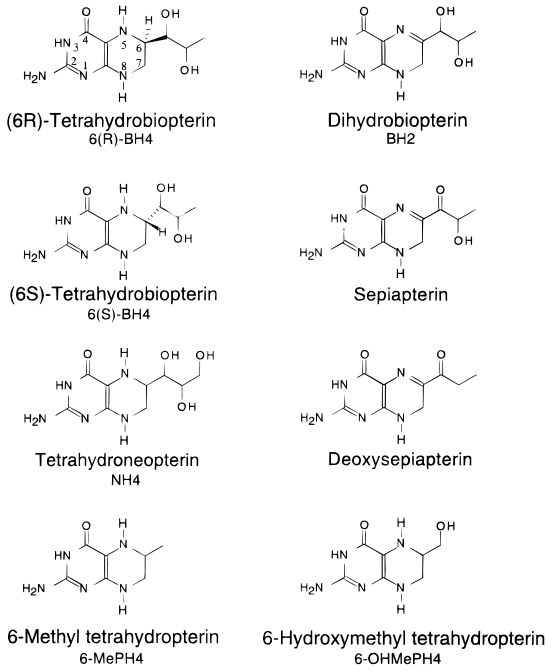

FIGURE 1: Structures, names, and abbreviations of the pterins used in this study. The numbering of the pterin ring atoms is shown for (6*R*)-BH4.

Enzyme Preparation. Mouse macrophage iNOS was purified from an *E. coli* strain coexpressing iNOS (N-terminal histidine$_6$-tagged) and calmodulin as described previously (*48*). Briefly, 1 L cultures of Terrific Broth containing 125 μg of ampicillin, 50 μg of chloramphenicol, and 4 mL of glycerol were initiated with 100 mL of overnight bacterial culture and shaken at 250 rpm at 37 °C. At OD_{600} of 0.8−1.0, protein expression was induced by addition of 1mM IPTG plus 0.4 mM δ-aminolevulinic acid, and the cultures were continuously shaken for 24−48 h at 25 °C. The cells were harvested by centrifuging at 5000 rpm for 15 min at 4 °C, and the pellet was resuspended in lysis buffer containing 40 mM EPPS (pH 7.6), 3 mM DTT, 250 mM sodium chloride, 1 mM L-arginine, 50 μg/mL lysozyme, and protease inhibitors [aprotinin/leupeptin and phenylmethanesulfonyl fluoride (PMSF)/pepstatin A]. The cells were ruptured by three successive freeze−thaw cycles followed by sonication (3 × 30 s) and then centrifuged for 20 min at 13 000 rpm and 4 °C. The supernatant was initially purified by an ammonium sulfate fractionation step (45% cut). The precipitate from this step was dissolved in a minimum volume of buffer as above minus the lysozyme and then applied to a Ni-NTA affinity column preequilibrated with buffer. The protein was eluted with 100 mL of 200 mM imidazole. The eluted protein was further purified by 2′,5′-ADP−Sepharose affinity chromatography as described previously (*35*, *49*),

except that the running buffer contained 0.5 mM L-arginine and no BH4. The NOS fraction was then concentrated and dialyzed twice with buffer containing 40 mM EPPS (pH 7.6), 10% glycerol, and 2.5 mM DTT to remove L-arginine.

L-Arginine Spectral Binding Constants. Spectral binding constants were determined for L-arginine binding to (6*R*)-BH4- or BH2-saturated iNOS at 25 °C. The pterin- and substrate-free enzyme was incubated at 4 °C overnight with 20 μM (6*R*)-BH4 or 150 μM BH2. The enzyme was diluted to approximately 4 μM in a volume of 350 μL with 40 mM EPPS, pH 7.6, and 10% glycerol. Imidazole (0.2 mM) was added to shift the iNOS heme iron to low-spin (*23*). Aliquots of concentrated L-arginine solution were added sequentially and spectra were recorded 15 and 20 min after each addition. Spectra were corrected for dilution. L-Arginine binding was determined as a Type I shift to high-spin heme iron by monitoring an increase in absorbance at 392 nm and a decrease in absorbance at 428 nm.

Enzyme Activity Measurements. The rate of NADPH oxidation by iNOS was determined in cuvettes at 340 nm assuming an $\epsilon_{340} = 6.22$ mM^{-1} cm^{-1}. The assay buffer contained 40 mM EPPS (pH 7.6), 0.3 mM DTT, 0.1 mg/mL BSA, 4 μM FAD, 4 μM FMN, 10 units/mL SOD, 100 units/mL catalase, and protease inhibitors. To 1.5 μg of enzyme was added the pterin and/or the substrate as required for each experiment, and the volume was brought to 300 μL with assay buffer. In some cases, relative NADPH oxidation rates for (6*R*)-BH4-bound and BH2-bound iNOS in the presence of various substrate analogues were estimated using a 96-well microplate and a Molecular Devices THERMOmax microplate reader using Molecular Device's Softmax software. NADPH consumption was followed at 37 °C by monitoring change in absorbance at 340 nm.

NO synthesis by a BH2-saturated iNOS was in one case measured at 25 °C using the spectrophotometric oxyhemoglobin method (Sennequier & Stuehr, 1996). A 300 μL reaction contained 40 mM EPPS (pH 7.6), 0.3 mM DTT, 1 mM NOHA or L-arginine, 150 μM BH2, 0.1 mg/mL BSA, 4 μM FAD, 4 μM FMN, 5 μM iNOS, 10 μM oxyhemoglobin, 10 units/mL SOD, 1300 units/mL catalase, and protease inhibitors. The reaction was initiated by adding 100 μM NADPH, and the NO-mediated conversion of oxyhemoglobin to methemoglobin was followed at 401 nm, using a difference extinction coefficient of 38 mM^{-1} cm^{-1}.

Time-course studies of NO and citrulline synthesis using the various pterin analogues and L-arginine or NOHA as substrate were done in assay buffer consisting of 40 mM EPPS (pH 7.6), 0.5 mg/mL BSA, 0.3 mM DTT, 1300 units/mL catalase, 150 units/mL SOD, 4 μM FAD, 4 μM FMN, and protease inhibitors. Substrate and pterin (final concentrations are given in the Results) were added to 1.8 μg of iNOS diluted in assay buffer to 150 μL total volume. NADPH (350 μM) was then added to initiate enzyme activity. Aliquots (15 μL) were removed from the assay at known time points and immediately acidified with 1 μL of concentrated HCl to terminate the reaction. The concentration of NO_2^- plus NO_3^- (both derived from spontaneous oxidation of NO in solution) was determined by chemiluminescence using the Sievers nitric oxide analyzer, Model NOA 280 (Sievers Instruments, Boulder, CO), using authentic sodium nitrite and sodium nitrate as standards. A 4-μL sample from each time point was injected into the NO analyzer radical purger, containing vanadium(III) and hydrochloric acid at 90 °C. Nitrite and nitrate in the sample are reduced to NO by V(III), and helium gas was used to purge NO from the solution for subsequent chemiluminescence detection. The citrulline concentration in each aliquot was determined by precolumn derivitization followed by reversed-phase HPLC and fluorescence detection as described elsewhere (*29*), with authentic L-citrulline used to prepare a standard curve. Samples were analyzed in duplicate in all cases.

Spectroscopic Measurements. Steady-state UV−visible absorption spectra and NADPH oxidation time scans were acquired on Hitachi U-2000 and U-3110 spectrophotometers controlled by the spectral acquisition and manipulation program SpectraCalc (Galactic Industries, Salem, NH). Pre-steady-state kinetic measurements were performed using a Hi-Tech Model SF-51 stopped-flow spectrometer. The rates of iNOS flavin and heme reduction were determined by rapid mixing of an anaerobic solution of 100 μM NADPH with an anaerobic solution containing 3 μM enzyme in 40 mM EPPS (pH 7.6) in the presence or absence of pterin cofactors [50 μM (6*R*)-BH4 or 150 μM BH2] and 5 mM L-arginine. Absorbance change was monitored at 485 nm for flavin reduction and at 440 nm for heme reduction in replicate experiments. Exponential fitting of the absorbance change over time was performed using software provided by the instrument manufacturer as previously described (*50*).

Subunit Dimerization. The ability of pterin analogues to promote dimerization of either full-length iNOS monomers or oxygenase domain monomers was done using methods previously described (*40*, *51*). The dimeric iNOS oxygenase domain with a histidine$_6$ tag at its carboxy terminus was overexpressed in *E. coli* and purified as previously reported (*41*, *52*). The iNOS oxygenase domain dimer was dissociated into monomers by dialysis for 90 min at 4 °C in 40 mM HEPES buffer (pH 7.5) containing 10% glycerol, 3 mM DTT, and 5 M urea, followed by 4-h dialysis in buffer containing 2 M urea, and finally overnight dialysis with buffer containing 0.1 M urea (*40*). Gel-filtration chromatography confirmed that this protocol resulted in >80% subunit dissociation. Dimerization of oxygenase domain monomers was performed by incubation of 1 μM enzyme at room temperature for 1 h in 40 mM HEPES (pH 7.5) containing 3 mM DTT, 0.05 mg/mL BSA, the required pterin, and in some cases L-arginine. The extent of dimerization was determined by gel-filtration chromatography using a Pharmacia Biotech Inc. (Piscataway, NJ) FPLC system and a Pharmacia Superdex 200 column using 40 mM HEPES (pH 7.5) plus 3 mM DTT as the running buffer and a flow rate of 0.5 mL/min (*40*).

Full-length pterin- and L-arginine-free iNOS was dissociated into monomers by incubation for 90 min at 37 °C in 40 mM EPPS (pH 7.6) containing 10% glycerol, 3 mM DTT, and 2 M urea (*51*). Dimerization was induced in the urea-incubated sample itself by incubating with a pterin alone or in some cases with L-arginine for 45 min at 25 °C. The extent of dimerization was estimated by determining NO synthesis activity following the dimerization reaction (*51*) using the oxyhemoglobin NO assay (*53*) at 37 °C. For this assay, 2 mL of the incubated sample was diluted in a cuvette to a total volume of 750 μL in 40 mM EPPS (pH 7.6) containing 0.3 mM DTT, 1 mg/mL BSA, 10 units/mL SOD,

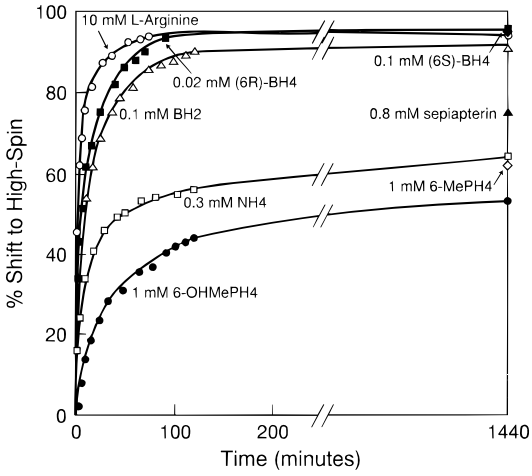

FIGURE 2: Heme iron spin shift associated with pterin binding to iNOS. The pterin- and substrate-free enzyme (3 μM) was incubated at 25 °C with each pterin or arginine at the specified concentrations, and its absorbance spectrum was acquired at periodic time intervals. The extent of spectral shift toward high spin was determined by the absorbance difference at 400 and 459 nm. A complete shift of 100% was designated for iNOS incubated with 10 mM L-arginine and 20 μM (6*R*)-BH4 for 2 h, after which time no further changes in absorbance were observed. The data points at 24 h were acquired from samples that were dialyzed in buffer containing the pterin of interest.

100 units/mL catalase, 4 μM FAD and FMN, 5 μM oxyhemoglobin, 1 mM L-arginine, 0.1 mM NADPH, and 25 μM (6*R*)-BH4. The NO-mediated conversion of oxyhemoglobin to methemoglobin over the first 5 min of the reaction was monitored at 401 nm and converted to a rate of NO synthesis using the difference extinction coefficient of $\epsilon_{401} = 38\ \text{mM}^{-1}\ \text{cm}^{-1}$.

RESULTS

Spectral Analysis of Pterin and L-Arginine Binding. Binding of each pterin or L-arginine to ferric iNOS was investigated spectroscopically by comparing their ability to cause a shift in heme iron spin state from low- to high-spin (increase in absorbance at 400 nm and decrease at 459 nm) over time. The results are shown in Figure 2, with a 100% shift representing that achieved upon incubating iNOS with both 20 μM (6*R*)-BH4 and 10 mM L-arginine, which causes a nearly complete shift to high-spin (*19*). In all cases examined, spectral change associated with binding occurred relatively slowly, requiring 2 h or more to approach equilibrium. After 24 h, samples that received L-arginine, (6*R*)-BH4, (6*S*)-BH4, or BH2 all achieved > 90% transition to high-spin, whereas samples receiving sepiapterin, NH4, 6-MePH4, or 6-OHMePH4 achieved intermediate transitions that ranged from 75% to 50% high-spin by 24 h, respectively.[2] For pterins that caused intermediate spin shift transitions, replicate experiments were done using higher pterin concentrations to test if saturating conditions had been achieved. The spin shift transitions obtained were identical in magnitude to those achieved at the lower concentrations (data not shown), indicating the original concentrations were sufficient to saturate iNOS. These concentrations were then used in the remainder of our studies unless specified otherwise.

Spectral binding constants were determined in the presence of 0.2 mM imidazole for L-arginine binding to iNOS containing (6*R*)-BH4 or BH2. Reciprocal plots of L-arginine concentration versus the Type I spectral shift obtained ($A_{392} - A_{428}$) gave spectral binding constants for L-arginine of $K_s = 12\ \mu$M with (6*R*)-BH4-bound iNOS and $K_s = 24\ \mu$M with BH2-bound iNOS. The similar affinity toward L-arginine is consistent with radioligand binding data that showed both BH2- and BH4-saturated iNOS exhibits a similar affinity toward N^{ω}-nitroarginine and in general exhibit a binding synergism between pterins and substrate or substrate analogues (*41*).

Pterin and L-Arginine Effects on NOS Catalysis. Specific rates of NO synthesis by iNOS reconstituted with the various pterins were determined by removing aliquots from reactions at known time points and analyzing for nitrite plus nitrate content by chemiluminescence and for citrulline content by HPLC.[3] As shown in Table 1, all tetrahydropterin analogues supported NO and citrulline synthesis from either L-arginine or NOHA at rates that matched those observed for iNOS saturated with (6*R*)-BH4. By contrast, the three dihydropterins supported no detectable NO or citrulline synthesis from either L-arginine or NOHA.

To determine if BH2 could support NO synthesis at a level below the detection limit of our normal assay, we used the oxyhemoglobin assay to measure NO synthesis in a reaction containing BH2-saturated iNOS at a concentration sufficient to detect NO synthesis due to a single catalytic turnover (5 μM iNOS). However, we observed no detectable NO synthesis from either L-arginine or NOHA in a 10 min reaction compared to a substrate-free control, indicating BH2 did not support NO synthesis even at this level of detection.

Rates of NADPH consumption by iNOS reconstituted with or without the various pterins are also shown in Table 1. The basal level of NADPH oxidation by a pterin- and L-arginine-free iNOS at 37 °C was 61 ± 5 nmol of NADPH min^{-1} (mg of enzyme)$^{-1}$ ($\sim$8 min^{-1} per monomer). Addition of a substrate-based inhibitor of heme iron reduction (thiocitrulline) did not alter the basal rate of NADPH oxidation, suggesting that it occurs independent of electron transfer to the iNOS heme iron (54). Adding either L-arginine or NOHA to pterin-free iNOS increased its NADPH consumption rate to 165 ± 1 and 300 ± 12 nmol of NADPH min^{-1} (mg of enzyme)$^{-1}$, respectively, indicating that substrates can increase iNOS NADPH consumption in the absence of bound pterin.

Adding (6*R*)-BH4 alone to iNOS increased its NADPH oxidation to 245 ± 1 nmol of NADPH min^{-1} (mg of enzyme)$^{-1}$. In marked contrast, the tetrahydropterin analogues NH4, 6-OHMePH4, and 6-MePH4 were found not to increase NADPH consumption by iNOS over the basal level, while (6*S*)-BH4 only caused a minor enhancement. The dihydropterins BH2, sepiapterin, and deoxysepiapterin each increased iNOS NADPH consumption to levels similar to that observed with (6*R*)-BH4. Increased NADPH oxidation associated with (6*R*)-BH4 or BH2 saturation was in both cases negated by thiocitrulline, suggesting that NADPH oxidation promoted by these pterins involves electron transfer to the iNOS heme iron.

[2] Spectra were recorded to determine the extent of iNOS heme iron spin shift to high-spin after 24 h dialysis of the enzyme with the pterin analogue of interest.

[3] The oxyhemoglobin NO trapping assay could not be used to measure NO synthesis because tetrahydropterins at the concentrations used in this study interfered with the assay.

Table 1: Enzymatic Activities of iNOS Reconstituted with Different Pterins

pterin	substrate[a]	pterin EC_{50} for NADPH oxidation[b] (μM)	NADPH oxidation[c] (nmol min^{-1} mg^{-1})	NO synthesis[c] (nmol min^{-1} mg^{-1})	citrulline synthesis[c] (nmol min^{-1} mg^{-1})
none	none		61 ± 5	0	0
	L-arginine		165 ± 1	0	0
	NOHA		300 ± 12	0	0
	thiocitrulline		69 ± 7	NA[d]	NA
(6*R*)-BH4	none	0.60	245 ± 1	0	0
	L-arginine	0.11	1270 ± 140	219 ± 4 (1520 ± 160)[e]	219 ± 7
	NOHA		390 ± 10	205 ± 3	210 ± 17
	thiocitrulline		69 ± 11	NA	NA
BH2	none	6.2	304 ± 7	0	0
	L-arginine		280 ± 30	0	0
	NOHA		291 ± 2	0	0
	thiocitrulline		79 ± 20	NA	NA
sepiapterin	none	50	131 ± 3	0	0
	L-arginine		281 ± 5	0	0
deoxysepiapterin	none	11	240 ± 4	0	0
	L-arginine		290 ± 40	0	0
(6*S*)-BH4	none		97 ± 5	0	0
	L-arginine	6.5	1260 ± 140	97 ± 5	90 ± 9
	NOHA		331 ± 12	124 ± 3	124 ± 10
NH4	none		60 ± 2	0	0
	L-arginine	100	1070 ± 120	223 ± 8	270 ± 20
	NOHA		415 ± 24	179 ± 7	190 ± 20
6-MePH4	none		65 ± 1	0	0
	L-arginine	59	1200 ± 120	210 ± 8	197 ± 15
	NOHA		360 ± 22	163 ± 5	190 ± 20
6-OHMePH4	none		56 ± 3	0	0
	L-arginine	89	1320 ± 120	202 ± 9	195 ± 25
	NOHA		327 ± 6	200 ± 10	270 ± 20

[a] Concentrations used were 5 mM L-arginine, 1 mM L-NOHA, and 1 mM thiocitrulline. [b] EC_{50} represents the pterin concentration at which 50% of maximal activity was obtained, as determined by double-reciprocal Lineweaver−Burk plots. [c] NADPH oxidation assays were done at 37 °C and the NO and citrulline synthesis assays were done at 25 °C. Values are the mean plus standard error of two determinations each. [d] This measurement is not applicable since thiocitrulline inhibits heme iron reduction and thus cannot support product synthesis. [e] This specific activity for NO synthesis was determined at 37 °C using the oxyhemoglobin method.

Addition of L-arginine to the (6*R*)-BH4-saturated iNOS boosted its rate of NADPH consumption, consistent with previous studies using BH4-replete iNOS isolated from mammalian cells (*27*). Because the rate increase is greater than the sum of the individual rates obtained with (6*R*)-BH4 or L-arginine, it identifies a synergism between the pterin and substrate in enhancing electron transfer through the enzyme. An increase in NADPH oxidation in response to L-arginine was also observed for iNOS saturated with each of four tetrahydropterin analogues. In contrast, iNOS saturated with any of the three dihydropterins did not significantly increase its NADPH consumption rate in response to L-arginine.

The inability of BH2-bound iNOS to increase its NADPH consumption in response to L-arginine was further investigated by examining its NADPH oxidation in response to a variety of substrate analogues that are known to (a) increase NADPH oxidation by BH4-replete iNOS while being metabolized to NO (NMA, homoarginine), (b) increase NADPH oxidation without being metabolized to NO (agmatine, *N*-hydroxyguanidine, AGPA), or (c) lower NADPH consumption without being metabolized to NO (thiocitrulline, SEITU, *N*-aminoguanidine) (*55*). The results are summarized in Figure 3. Of five substrate analogues that increased NADPH oxidation by (6*R*)-BH4-bound iNOS, only two (*N*-hydroxyguanidine and AGPA) increased NADPH oxidation by the BH2-saturated iNOS. NMA did not significantly affect its NADPH consumption rate, while L-arginine, homoarginine, and agmatine moderately inhibited NADPH consumption relative to substrate-free BH2-bound iNOS. L-Thiocitrulline or SEITU inhibited NADPH oxidation by (6*R*)-BH4-saturated and by BH2-bound iNOS to identical degrees, while *N*-aminoguanidine only inhibited NADPH consumption by the (6*R*)-BH4-saturated iNOS and did not appreciably affect BH2-saturated iNOS. By comparison, an iNOS saturated with NH4 responded to the substrate analogues in a qualitatively identical manner as a (6*R*)-BH4-saturated iNOS regarding their positive or negative effects on NADPH oxidation rate (data not shown). This suggests that the divergent response seen for BH2 is related to a difference in oxidation state relative to BH4.

Effect of Pterins and L-Arginine on iNOS Heme Iron Reduction. Spectral analyses of heme iron reduction in iNOS samples saturated with various pterins are presented in the multiple panels of Figure 4, with the results summarized in Table 2. These experiments were performed under anaerobic conditions in CO-saturated buffer such that iNOS heme iron reduction would lead to formation of the ferrous−CO complex, which absorbs at 444 nm (*49*, *56*). For each experiment a concentrated sample of iNOS was incubated overnight at 4 °C with the pterin of interest (± L-arginine) to assure binding equilibrium.

For pterin-free iNOS (panel A), addition of excess NADPH decreased absorbance from 390 to 500 nm and between 600 and 650 nm, indicating reduction of the iNOS flavins (*27*). However, no spectral signal at 444 nm was

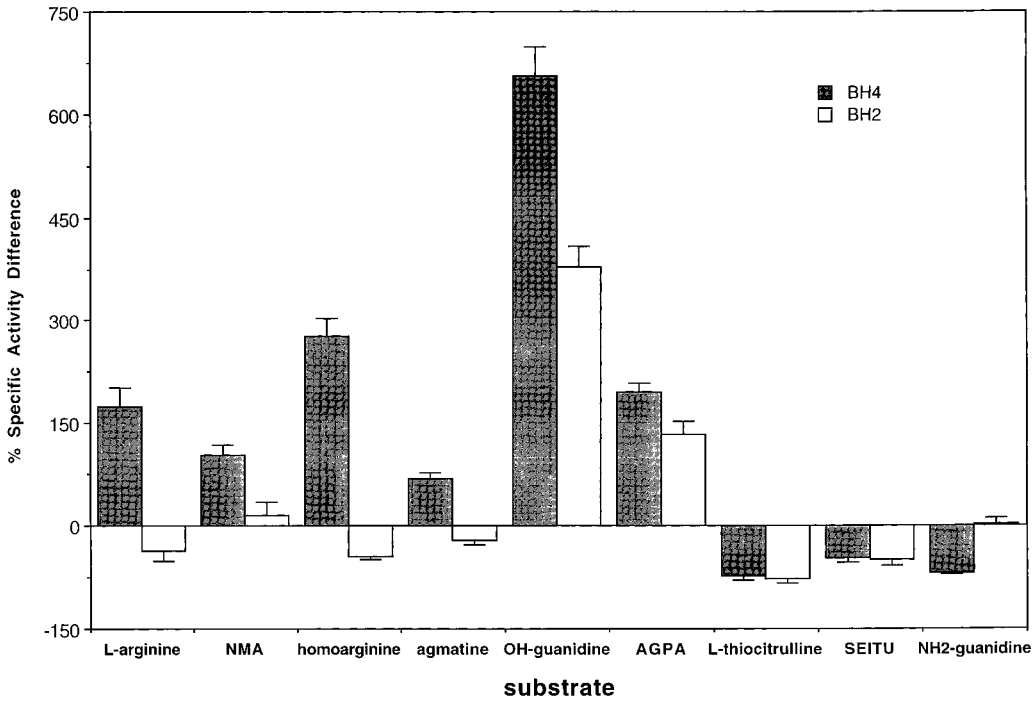

FIGURE 3: Effect of substrate analogues on the rate of NADPH oxidation for (6*R*)-BH4-bound iNOS and BH2-bound iNOS. The data represent the percent difference in specific activities between the pterin-bound enzyme in the presence or absence of each particular substrate analogue. NADPH consumption was monitored at 340 nm using a 96-well microplate reader as described in Materials and Methods. The data shown are means and standard deviations of three experiments done in duplicate. The concentrations used were 4 μM iNOS, 20 μM (6*R*)-BH4, 150 μM BH2, 2 mM L-arginine, 0.5 mM NMA, 1 mM homoarginine, 0.5 mM agmatine, 5 mM *N*-hydroxyguanidine, 1 mM AGPA, 0.2 mM thiocitrulline, 0.2 mM SEITU, and 0.5 mM aminoguanidine.

observed, indicating that heme iron reduction did not occur. Subsequent addition of L-arginine to pterin-free iNOS resulted in an immediate and intense signal at 444 nm, indicating that L-arginine alone could trigger reduction of the iNOS heme iron as mediated by the iNOS flavins. The extent of NADPH-dependent heme iron reduction was estimated as in Siddhanta et al. (*52*) by comparing the absorbance difference obtained at 444−500 nm after NADPH addition and after adding excess sodium dithionite to completely reduce the sample (panel B). By this method, approximately 80% of the heme iron was judged reducible by NADPH in the presence of L-arginine alone. A similar experiment performed with NOHA instead of L-arginine showed it also supported NADPH-dependent heme iron reduction in iNOS on its own (data not shown).

Addition of excess NADPH to (6*R*)-BH4-saturated iNOS (panel C) generated a major peak at 444 nm and left a minor peak at 421 nm. The 444-nm signal represents the cysteine-ligated six-coordinate ferrous−CO complex (*37*), while the signal at 421 nm represents a five-coordinate ferrous−CO complex in which the cysteine ligand has been weakened or dissociated from the heme iron (*57*). The extent of NADPH-dependent heme iron reduction as judged by the absorbance of the 444-nm band was estimated to be ∼80%. In the presence of both (6*R*)-BH4 and L-arginine (panel D), addition of excess NADPH resulted in complete reduction of the iNOS heme iron and exclusive formation of the six-coordinate ferrous−CO complex, as previously observed (*54*).

Identical experiments were performed using pterins that differed in their abilities to promote NADPH oxidation or NO synthesis relative to (6*R*)-BH4. Panel E shows the results for NADPH reduction of BH2-saturated iNOS. As for the (6*R*)-BH4-bound enzyme, addition of excess NADPH led to development of spectral bands at 421 and 444 nm, indicating heme iron reduction had occurred. Formation of the cysteine-ligated ferrous−CO species was ∼90% of maximal. Thus, the extent of heme reduction achieved for the BH2-saturated iNOS was equivalent to or slightly greater than that obtained with (6*R*)-BH4-saturated iNOS. In the presence of L-arginine, the BH2-saturated iNOS formed the cysteine-bound ferrous heme−CO complex almost exclusively (panel F) with ∼90% of the heme iron being reduced. Unfortunately, preparations of iNOS saturated with sepiapterin or deoxysepiapterin could not be analyzed in this manner due to their strong absorbance in the visible region.

For iNOS saturated with (6*S*)-BH4 (spectral data not shown; results summarized in Table 2), addition of excess NADPH primarily formed the six-coordinate ferrous−CO species with the extent of heme reduction estimated at 45% maximal. When both (6*S*)-BH4 and L-arginine were present we observed exclusive formation of the six-coordinate ferrous−CO complex with ∼65% of the heme being reduced.

Panel G contains spectra of iNOS saturated with NH4. The initial spectrum was recorded prior to NADPH addition and contains a very broad Soret absorbance composed of a band centered at 395 nm, which is due to high-spin ferric heme, and an equally intense band centered at 417 nm, which is due to low-spin ferric heme (*23*). Addition of excess NADPH resulted in buildup of a small absorbance peak at 422 nm and no peak at 444 nm, suggesting little or no heme iron reduction occurred. A lack of heme iron reduction is also evidenced by the continued presence of ferric heme bands in the 500−650 nm region of the spectrum following NADPH addition. After addition of L-arginine, the 444-nm peak characteristic of the six-coordinate ferrous−CO com-

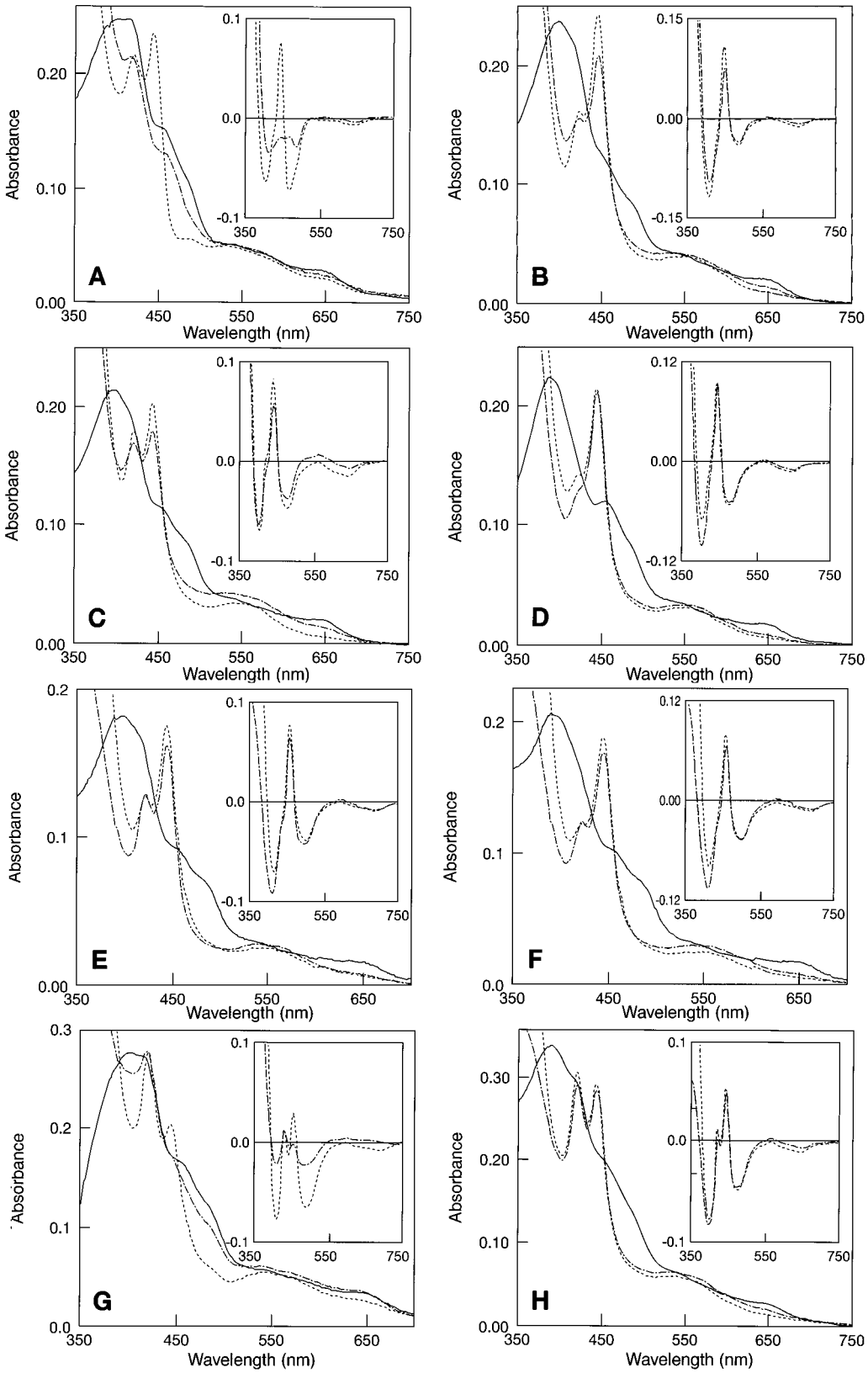

FIGURE 4: Absorbance spectra of iNOS showing the effects of individual pterins and L-arginine on the characteristics of iNOS heme reduction by NADPH. All experiments were performed in CO-saturated 40 mM EPPS (pH 7.6). Inset figures represent the difference spectra from the initial spectrum in each panel. (A) Solid line, pterin- and arginine-free iNOS; dashed−dotted line, after addition of 50 mM NADPH; dotted line, after addition of 5 mM L-arginine. In panels B−F, the solid line represents the spectrum of the initial enzyme with the particular pterin and/or L-arginine, the dashed−dotted line is the spectrum taken after addition of excess NADPH, and the dotted line is the spectrum taken after addition of excess sodium dithionite. (B) iNOS plus 5 mM L-arginine; (C) iNOS plus 20 μM (6*R*)-BH4; (D) iNOS plus 20 μM (6*R*)-BH4 and 5 mM L-arginine; (E) iNOS plus 150 μM BH2; (F) iNOS plus 150 μM BH2 and 5 mM L-arginine. (G) Solid line, iNOS plus 600 μM NH4; dashed−dotted line, following addition of excess NADPH; dotted line, after addition of 5 mM L-arginine. (H) solid line, iNOS plus 600 μM NH4 and 5 mM L-arginine; dashed−dotted line, after addition of excess NADPH; dotted line, after addition of excess sodium dithionite. Data shown are representative of two or three individual experiments.

Table 2: Extent of NADPH-Dependent Heme Iron Reduction in iNOS in the Absence or Presence of Pterins and L-Arginine[a]

	extent of heme iron reduction[b] (% reduced)		presence of 422-nm signal[c]	
pterin	−L-arginine	+L-arginine	−L-arginine	+L-arginine
none	0	80		minor
50 μM (6*R*)-BH4	80	~100	yes	minor
150 μM BH2	90	90	yes	minor
300 μM (6*S*)-BH4	45	65	yes	minor
600 μM NH4	very little	> 90	yes	major
1 mM 6-OHMePH4	very little	>90	yes	major

[a] Pterins were added to iNOS in the presence or absence of L-arginine in an air-tight cuvette and incubated for 1 h at 4 °C under a stream of argon. CO-saturated buffer was then added to a total volume of 350 μL. The final concentrations were approximately 3 μM iNOS, 5 mM L-arginine, and the given concentration of pterin. After an initial absorbance spectrum was acquired, NADPH (60 μM) was added, the spectrum of the NADPH-reduced iNOS was collected, excess sodium dithionite was then added, and the final spectrum of the fully reduced enzyme was recorded. Data are representative of at least two replica experiments. [b] The extent of heme iron reduction was estimated by the equation $100\%[(A_{444} - A_{500})_{NADPH}/(A_{444} - A_{500})_{dithionite}]$, where the subscripts NADPH and dithionite indicate the reductant used prior to each scan. [c] The 422-nm absorbance is associated with formation of a five-coordinate cysteine-dissociated ferrous−CO complex (Martinis et al., 1996).

plex formed as a minor component that was overshadowed by a 422-nm peak that is characteristic of a five-coordinate ferrous−CO complex (*57*). Addition of NADPH to an iNOS saturated with both NH4 and L-arginine (panel H) produced peaks of equal intensity at 422 and 444 nm, indicating NADPH could support substantial heme iron reduction in this circumstance to generate both five- and six-coordinate ferrous−CO complexes. Adding dithionite led to small changes in the spectrum, suggesting that greater than 90% of the heme iron was reduced by NADPH. Results obtained with 6-OHMePH4-saturated iNOS were similar to those obtained for the NH4-saturated enzyme in both the presence and absence of L-arginine (spectral data not shown; summarized in Table 2).

Kinetics of Heme Iron Reduction. The above results show that (6*R*)-BH4, BH2, or L-arginine enabled NADPH-dependent reduction of the iNOS heme iron. We next determined how these molecules would affect the rate of heme iron reduction. Experiments were performed in a CO-free anaerobic environment. Figure 5 shows the spectral changes observed upon NADPH reduction of iNOS containing (6*R*)-BH4 and L-arginine. Flavin reduction was evidenced by a decrease in absorbance at 485 nm, while heme iron reduction was indicated by a decrease in absorbance at 400 nm and an increase at 440 and 570 nm. Similar spectral changes were observed in an experiment containing BH2 in place of (6*R*)-BH4 (data not shown). A control experiment in which the oxygenase domain of iNOS (which does not contain flavins) was reduced with dithionite confirmed that the increase in absorbance centered at 440 nm is primarily due to heme iron reduction (data not shown). Therefore, we monitored NADPH-dependent reduction of iNOS flavin and heme groups by following the absorbance change over time at 485 and 440 nm, respectively. Time scans obtained at both wavelengths are shown in Figure 6 for iNOS saturated with (6*R*)-BH4 and L-arginine. The 440-nm time scan is

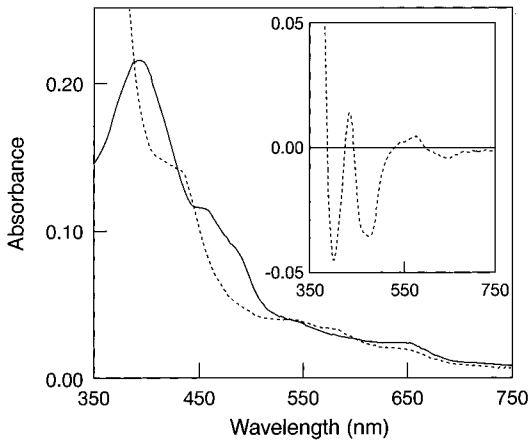

FIGURE 5: Absorbance spectra of oxidized and reduced (6*R*)-BH4-saturated iNOS. Spectra were collected under anaerobic conditions before (solid line) and after adding excess NADPH (dotted line). The inset shows the reduced minus oxidized difference spectrum.

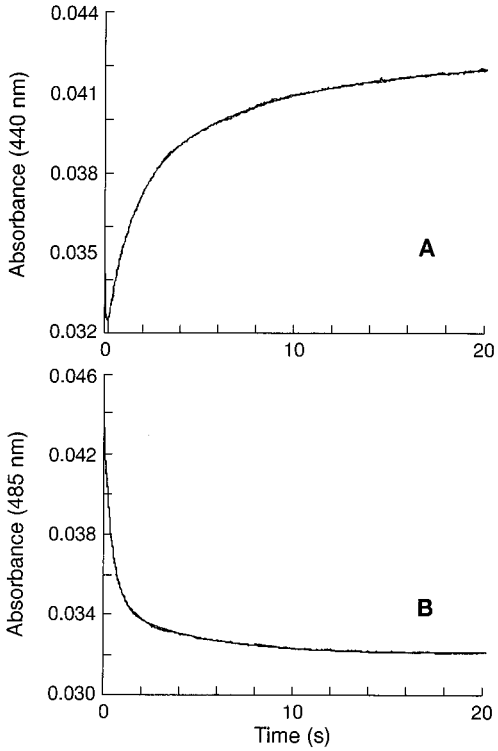

FIGURE 6: Kinetics of NADPH reduction of (6*R*)-BH4-saturated iNOS as monitored by stopped-flow spectroscopy. The reaction was initiated by mixing of an anaerobic buffered solution containing iNOS and (6*R*)-BH4 with an anaerobic solution containing NADPH. The absorbance change at 440 nm was monitored to determine the rate of heme reduction (A) and at 485 nm to determine the rate of flavin reduction (B) by NADPH. The scans shown are representative of 5−10 repetitive scans.

biphasic due to overlapping flavin absorbance, which gives an initial decrease in absorbance at 440 nm that represents NADPH-dependent reduction of the flavins (*50*).

The pseudo-first-order rate constants for iNOS flavin and heme iron reduction by NADPH under various conditions are listed in Table 3. Adding L-arginine or pterins did not appreciably alter the rate of flavin reduction. However, they each enabled heme iron reduction which was otherwise not observed under pterin- and substrate-free conditions. When added singly, L-arginine supported the fastest rate of heme iron reduction, followed by BH2, then BH4. Indeed, the

Table 3: First-Order Rate Constants for the Reduction of iNOS Flavins and Heme Iron by NADPH[a]

pterin	L-arginine	flavin reduction (s^{-1})	heme reduction (s^{-1})
none	no		not observed
	yes	4.0 ± 0.1	0.98 ± 0.02
50 μM (6*R*)-BH4	no	4.1 ± 0.1	0.18 ± 0.02
	yes	4.8 ± 0.1	0.86 ± 0.02
150 μM BH2	no	3.5 ± 0.2	0.47 ± 0.03
	yes	3.9 ± 0.2	1.29 ± 0.02

[a] Rate constants were determined by mixing an anerobic buffered solution containing 3−3.5 μM iNOS, the desired pterin, and 10 mM L-arginine (where indicated) with an anaerobic solution of 100 μM NADPH. The pterin concentrations are those obtained after mixing. Flavin and heme iron reduction were monitored at 485 and 440 nm, respectively. Values are the mean ± SD from 5−10 individual scans.

Table 4: Promotion of iNOS Oxygenase Domain Dimerization by Pterin Analogues with and without Substrate[a]

pterin	pterin (mM)	L-arginine (mM)	extent of dimerization (%)
(6*R*)-BH4	0.01	0	> 80
(6*S*)-BH4	0.01	0	20
		1	>80
BH2	0.1	0	80
sepiapterin	0.1	0	20
		0.3	80
	1	0	80
deoxysepiapterin	0.1	0	>80
NH4	0.6	0	40
		1	80
6-MePH4	1	0	40−50
		1	>80
6-OHMePH4	1	0	40−50
		1	>80

[a] The dimeric iNOS oxygenase domain was dissociated into monomers as described in Materials and Methods. The extent of dimer reassembly promoted by the pterin, with and without L-arginine, was estimated by gel-filtration chromatography. The monomer preparation was estimated to contain 20% residual dimer. L-Arginine at 1 mM alone was not sufficient to promote dimerization of the iNOS oxygenase monomers. Data are representative of two similar experiments.

rate of heme iron reduction in BH2-saturated iNOS was 2−3 times faster than in a (6*R*)-BH4-saturated iNOS. Addition of L-arginine to either BH2- or (6*R*)-BH4-saturated iNOS samples further increased the rate of heme iron reduction in both cases.

iNOS Subunit Reassociation. Although BH4 can promote dimerization of both full-length and oxygenase domain monomers (*35*, *39*, *40*), nothing is known about the structural specificity of this process. We therefore examined the capacity of each pterin to promote dimerization of both iNOS oxygenase and full-length monomers. Table 4 summarizes the results of experiments where iNOS oxygenase domain monomers were incubated with each pterin ± L-arginine and the extent of dimerization was assessed by gel-filtration chromatography. Certain pterins [(6*R*)-BH4, BH2, deoxysepiapterin] promoted extensive dimerization on their own, while others (sepiapterin, NH4, 6-MePH4, or 6-OHMePH4) promoted a lesser extent of dimerization. Adding individual pterins plus L-arginine (0.1 or 1 mM)[4] enabled almost complete dimerization in all cases tested.

[4] L-Arginine added alone at 1 mM promoted less than 20% dimerization in this assay system.

Table 5: Promotion of Full-Length iNOS Subunit Dimerization by Pterins in the Presence and Absence of Substrate[a]

pterin	substrate	NO synthesis activity [nmol min^{-1} (mg of enzyme)$^{-1}$]	% full-length reassembly[b]
none	none	280 ± 10	18 ± 3
20 μM (6*R*)-BH4	none	1240	82 ± 9
150 μM BH2	none	870	57 ± 6
600 μM NH4	none	590	39 ± 4
600 μM NH4	1 mM L-arginine	1180	78 ± 8
1.0 mM sepiapterin	none	930	61 ± 6
1.0 mM sepiapterin	1 mM L-arginine	1250	82 ± 9

[a] Dimerization of full-length iNOS monomers was promoted by incubation with the various pterins with or without L-arginine. The extent of dimer reassembly was estimated by the recovery of NO synthesis as determined using the oxyhemoglobin assay at 37 °C. The pterin-treated enzyme samples were diluted into a buffer solution containing excess (6*R*)-BH4, L-arginine, and NADPH and the assay run as described in Materials and Methods. [b] Relative to a NO synthesis specific activity for dimeric full-length iNOS of 1520 ± 160 nmol NO/minute/mg enzyme.

The ability of certain pterins to promote dimerization of full-length iNOS monomers was assessed by measuring the recovery of NO synthesis activity (*35*, *55*) and is summarized in Table 5. Full-length iNOS monomers incubated with no pterin or with 1 mM L-arginine alone achieved a specific activity of 280 ± 10 nmol of NO min^{-1} (mg of enzyme)$^{-1}$, which indicates that 18% ± 3% of iNOS was dimeric at the end of these incubations [based on a V_{max} activity for the parent full-length iNOS dimer of 1520 ± 160 nmol of NO min^{-1} (mg of enzyme)$^{-1}$ at 37 °C]. In the absence of L-arginine, (6*R*)-BH4 promoted the greatest amount of dimerization, followed by sepiapterin, BH2, and NH4. As seen for the iNOS oxygenase domain, the presence of pterin plus L-arginine further increased dimerization of full-length iNOS monomers.

DISCUSSION

Availability of dimeric, pterin-free iNOS (*48*) allowed reconstitution of the enzyme with a variety of non-native dihydro- and tetrahydropterins to investigate how each influences the structure-function of iNOS. As discussed below, the pterin-free and -reconstituted enzymes exhibited a number of surprising similarities and differences that, when viewed together, increase our understanding of BH4 function in iNOS.

Unique Properties of Pterin-Free iNOS. The pterin-free iNOS was distinguished by being primarily dimeric and containing heme iron in a mixture of high- and low-spin states. The former property contrasts overexpression of full-length iNOS in bacteria from its normal expression in mammalian cells, which requires BH4 to form significant amounts of dimer (*39*). The latter property distinguishes expression of the full-length enzyme from its oxygenase domain (amino acids 1−498), which is isolated as a dimer that contains only low-spin heme iron (*41*). The high-spin component in our full-length iNOS apparently does not result from L-arginine contamination, because other than a partial high-spin character it exhibited no properties of an L-arginine-bound form. We found that pterin-free iNOS was completely inactive regarding NO synthesis from either L-arginine or NOHA but could reconstitute its NO synthesis after incuba-

tion with any of five tetrahydropterins. This indicates that full-length iNOS can properly fold before incorporating pterin and confirms what had previously been surmised from work using pterin-deficient enzymes (*30*, *32*, *33*); namely, a tetrahydropterin must be present to support NADPH-driven NO synthesis by iNOS.

A Role for Pterin and Substrate in Supporting Heme Iron Reduction. The pterin-free iNOS exhibited a defect of clear functional significance—it was unable to transfer NADPH-derived electrons to its heme iron unless reconstituted with (6*R*)-BH4, L-arginine, or certain other pterins. This identifies a novel role for BH4 or L-arginine in supporting electron transfer between the iNOS flavins and heme. Work done previously with BH4-replete NOS enzymes had shown that the flavin-to-heme electron transfer requires bound calmodulin (*27*, *58*) and enzyme dimeric structure (*51*, *52*). We can now conclude that for iNOS these two posttranslational modifications are necessary but in the absence of BH4 or L-arginine are insufficient for heme iron reduction as catalyzed by the reductase domain. Because (6*R*)-BH4 and L-arginine stabilize the high-spin state of iNOS and alter the heme environment in other ways (*28*, *36*, *41*, *59*), we speculate that binding either molecule might increase the reduction potential of the iron relative to the flavins and make electron transfer to the heme thermodynamically favorable. A thermodynamic model is attractive, based on work done with cytochrome P-450s that shows the degree of high-spin character achieved upon substrate binding can be correlated with the reducibility of the heme group (*60*−*62*). In contrast to iNOS, recent evidence suggests that neuronal NOS may be capable of catalyzing NADPH-dependent heme iron reduction even in the absence of bound BH4 or L-arginine (*63*), implying a fundamental difference may exist between the NOS isoforms regarding control of heme iron reduction.

Structural Elements Important for Pterin Binding and Function. It is useful to consider how the two main elements of the biopterin molecule—namely, the oxidation state of its ring structure (7,8-dihydro versus 5,6,7,8-tetrahydro) and the composition/stereochemistry of the aliphatic side chain attached to the ring at the sixth position—influence the binding and functioning of the molecule. For iNOS, the properties most affected by changes in side-chain composition/stereochemistry and least affected by pterin ring oxidation state were the binding affinity, magnitude of the high-spin shift obtained upon binding, capacity to support heme iron reduction, capacity to stabilize the six-coordinate ferrous−CO complex, and ability to promote subunit dimerization. For each of these five functions, partial deletion of the side chain (6-MePH4, 6-OHMePH4) or addition of an extra hydroxyl group (NH4) caused greater perturbation than changing the stereochemistry at the sixth position (6S-BH4), substituting a side-chain carbonyl for a hydroxyl (sepiapterin), or additionally removing another side-chain hydroxyl group (deoxysepiapterin). That a similar structure−activity relationship is seen for all five functions suggests they arise through a common interaction between the pterin side chain and iNOS.

Although we obtained our pterin binding information indirectly by measuring the concentration-dependent effect of each pterin on iNOS NADPH oxidation rate, our conclusions regarding relative affinities are entirely consistent with recent direct measurements of pterin binding to neuronal NOS or iNOS (*33*, *41*) and will not be further discussed. Regarding the other four functions, it is remarkable that heme iron reduction and stabilization of a six-coordinate ferrous−CO species are only affected by side-chain composition and independent of ring oxidation state. Apparently, these two functions are sensitive to binding geometry as influenced by the side chain or to associated structural changes within iNOS and are insensitive to the electronic state of the pterin ring.

Three tetrahydropterins (NH4, 6-MePH4, and 6-OHMePH4) were unable to support NADPH-dependent heme iron reduction despite their stabilizing a considerable (40−60%) proportion of the heme iron in its high-spin state. Thus, changes brought on when the heme iron undergoes a high-spin shift cannot by themselves account for BH4's ability to support electron transfer to the heme. Their collective inability to support heme iron reduction also explains why NADPH oxidation rates by iNOS samples saturated with these three tetrahydropterins remained at the basal level of pterin-free iNOS. Although they each allowed NADPH-dependent heme iron reduction to occur if L-arginine was also present, this led to considerable formation of a five-coordinate ferrous−CO species instead of the six-coordinate thiol-ligated ferrous−CO complex that is normally seen with (6*R*)-BH4-saturated iNOS. Given that iNOS saturated with L-arginine alone forms a six-coordinate ferrous−CO complex, the results imply that the three tetrahydropterin analogues promote a weakening of the axial Fe−S bond and stabilize the five-coordinate CO complex of iNOS, whose formation is usually associated with enzyme inactivation (*37*, *64*). In spite of this, all tetrahydropterin analogues supported NO synthesis that was fully coupled to NADPH oxidation and proceeded at rates that matched an iNOS saturated with (6*R*)-BH4. In order for this to occur, we speculate that the analogous six-coordinate ferrous−O_2 (*28*) and ferrous−NO (*42*, *50*, *65*) complexes that form during iNOS catalysis must remain six-coordinate, or instead reversibly convert between a five- and six-coordinate form (ferrous−NO complex only). Although additional work is required to resolve how tetrahydropterins can stabilize different coordination states of the ferrous iron while still supporting NO synthesis, it is interesting to note that a five-coordinate ferrous−CO iNOS complex forms in the presence of the inhibitor ADT, and it can convert to a six-coordinate ferrous−CO species upon displacement of the inhibitor with excess L-arginine (*64*). This identifies one case where ferrous iNOS is able to reversibly change the coordination state of its heme iron.

All of the pterins studied were capable of promoting iNOS dimer assembly either alone or in combination with L-arginine. There was only a weak indication that dimerization might be dependent on pterin side-chain composition, given that some of the analogues with abbreviated side chains appeared less capable than others in promoting subunit association on their own. Tolerance toward change in pterin structure and electronic state is reminiscent of the low level of structural specificity observed for dimerization promoted by L-arginine and guanidine analogues (*55*), suggesting for both pterin and substrate simple binding site occupancy is sufficient to drive iNOS subunit dimerization.

Only two iNOS functions were dependent on the oxidation state of the pterin ring: the ability to support NO synthesis and the capacity to change NADPH oxidation rate in response to substrate or substrate analogue binding. Our data using pterin-free iNOS confirm that there is an absolute requirement for fully reduced pterin in NADPH-dependent NO synthesis. However, it was unexpected that all five tetrahydropterins we tested would prove equivalent in supporting the reaction. Their equivalence underscores an independence toward pterin side-chain composition or stereochemistry. Although the oxidation state of the ring appears to be the primary feature that determines if a pterin can support NO synthesis, it is interesting to note that at least one tight-binding tetrahydropterin analogue (4-aminotetrahydrobiopterin) does not support NO synthesis by iNOS or neuronal NOS (*38*, *66*). In addition, energy minimization calculations predict the geometry of the pterin ring structure differs greatly between the tetrahydro and dihydro states, with tetrahydropterin capable of existing in two energetically equivalent nonplanar conformations.[5] Whether such structural differences contribute to the tetrahydropterin requirement in NO synthesis is presently unknown.

A New Specific Function for BH4. We observed a surprising difference in the catalytic properties of iNOS reconstituted with dihydropterins versus tetrahydropterins; namely, only the latter group was able to increase its NADPH consumption rate in response to L-arginine. The inability of BH2 to support a substrate-induced increase in NADPH consumption is unique because BH2 otherwise enabled iNOS to respond normally toward L-arginine. This represents only the second case where BH2 differs from BH4 regarding an effect on NOS (the first is in supporting NO synthesis). The inability of BH2-saturated iNOS to respond to L-arginine in this manner is remarkable when one considers that for BH4-saturated iNOS, L-arginine triggers a 5-fold increase in NADPH oxidation rate even though a majority of the enzyme is present as an inactive ferrous−NO complex during the rate measurement because of NO synthesis (*50*, *65*). For BH2-saturated iNOS, a ferrous−NO complex cannot form during NADPH oxidation in the presence of L-arginine because NO is not made. Thus, all things being equal, one would expect NADPH consumption in response to L-arginine to rise to much higher levels in the BH2- versus BH4-saturated iNOS. Understanding why this does not occur may help reveal why only tetrahydropterins can support NO synthesis.

Although the BH2-saturated iNOS did not change its NADPH oxidation rate in response to L-arginine, this defect was not absolute because it extended to most but not all of the L-arginine and guanidine analogues we examined. Although this response pattern is complex, it is consistent with L-arginine and analogues adopting at least four distinct binding modes in NOS (*26*) and supports our current data that show interactions with bound substrate still occur at some level in the BH2-saturated enzyme. As discussed in a previous publication (*55*), several L-arginine and guanidine analogues can increase NADPH oxidation by iNOS above the basal rate without serving as a substrate for NO synthesis. In such cases, the increase in NADPH oxidation reflects an increase in electron transfer from the enzyme's heme iron to O_2. Other substrate analogues can actually lower the rate of iNOS NADPH oxidation below the basal level by directly inhibiting heme iron reduction (*54*). In our current study, we saw that only two of the six analogues which stimulate NADPH consumption by BH4-saturated iNOS could also increase NADPH oxidation by the BH2-bound enzyme, while two of the three analogues known to inhibit NADPH consumption by BH4-bound iNOS also inhibited NADPH consumption by BH2-saturated iNOS. This suggests that the mechanism responsible for increasing electron transfer from iNOS to O_2 in response to substrate (or substrate analogues) may be more sensitive to the oxidation state of the pterin ring than is substrate-based inhibition of electron flux. The two analogues that inhibited electron flux through BH2- and BH4-bound iNOS (thiocitrulline and SEITU) may act by lowering the reduction potential of the heme iron[6] and thus prevent its reduction (*54*). Apparently, these analogues inhibit heme iron reduction independent of the oxidation state of the bound pterin. Whether substrate-induced increases in NADPH oxidation rate are likewise associated with positive changes in heme iron potential is unknown and will require further study.

Our current findings limit the number of possible points where tetrahydropterins might manifest their unique capacity to support NO synthesis. Consider that catalysis by dimeric iNOS includes (a) steps leading to and including heme iron reduction, (b) O_2 binding to the ferrous heme iron and its stepwise activation, (c) substrate interaction with reactive oxygen and subsequent oxygenation, and (d) product release, along with a return of the heme iron to its starting ferric state. On the basis of our current work, we now can state that all steps prior to and including heme iron reduction, such as iNOS dimer assembly, substrate binding, spin state change, and flavin reduction, are fundamentally the same for iNOS containing either tetra- or dihydrobiopterins. Therefore, the unique requirement for tetrahydropterins [and specifically (6*R*)-BH4] must be at a step beyond heme iron reduction. Of the subsequent steps noted in b−d above, we can probably exclude O_2 binding to the heme because CO, a molecular mimic for O_2, clearly binds to ferrous NOS in the presence or absence of L-arginine, BH2, or (6*R*)-BH4. However, it is still possible that individual pterins might support different rates of O_2 binding to and dissociation from the iNOS heme. Such differences could help explain why L-arginine only increases the rate of NADPH oxidation in tetrahydropterin-saturated iNOS. Regarding NO synthesis, we can only speculate what point(s) beyond O_2 binding are uniquely affected by (6*R*)-BH4. Recently, (6*R*)-BH4 has been shown to dramatically reduce the stability of the NOS ferrous−O_2 complex (*28*), suggesting tetrahydropterins can modulate the reactivity of iron-oxy species formed during catalysis. This has important implications for the second step of NO synthesis, because single-turnover studies with a (6*R*)-BH4-saturated NOS suggest that the ferrous−O_2 species reacts directly with enzyme-bound NOHA to generate citrulline and NO (*29*). As discussed above, the ferrous−O_2 species surely forms after heme iron reduction in either dihydro- or tetrahydropterin-saturated iNOS. However, this presents a paradox: why does the ferrous−O_2 species react with NOHA to generate products only in the tetrahydropterin-saturated

[5] J. Wang, personal communication.

[6] A. Presta and D. J. Stuehr, unpublished results.

enzyme? The current work should help construct experiments that can address and potentially solve this paradox.

SUMMARY

The dihydro- and tetrahydropterins exhibited a diverse capacity to support seven functions in iNOS that are modulated by (6*R*)-BH4 and important for NO synthesis. Five of these functions (pterin binding affinity, ability to shift the heme iron to its high-spin state, stabilization of the ferrous heme iron coordination structure, allowing NADPH-dependent heme iron reduction, and promoting iNOS subunit assembly) were supported by either dihydro- or tetrahydropterins, indicating the pterin cofactor fulfills these multiple roles independent of its ring oxidation state. On the other hand, two related catalytic functions (NO synthesis and NADPH consumption in response to substrates) required fully reduced (tetrahydro-) pterins. Only the natural cofactor (6*R*)-BH4 supported all seven functions to their maximal extent. These results identify a new role for (6*R*)-BH4 in modulating electron flux through iNOS in response to substrates and reveal that the tetrahydropterin must fulfill its unique function at a step in catalysis that follows heme iron reduction.

ACKNOWLEDGMENT

We thank Pam Clark and Jingli Zhang for technical assistance and Drs. Takao Kaneko and Kohsaku Uetani for performing the NO analysis.

REFERENCES

1. Griffith, O. W., & Stuehr, D. J. (1995) *Annu. Rev. Physiol. 57*, 707−736.
2. Ignarro, L., & Murad, F., Eds. (1995) *Advances in Pharmacology, Volume 34. Nitric Oxide: Biochemistry, molecular biology, and therapeutic implications*, Academic Press, San Diego, CA.
3. MacMicking, J., Xie, Q.-W., & Nathan, C. (1997) *Annu. Rev. Immunol. 15*, 323−350.
4. Forstermann, U., Gath, I., Schwarz, P., Closs, E. I., & Kleinert, H. (1995) *Biochem. Pharm. 50*, 1321−1332.
5. Xie, Q.-W., Cho, H. J., Calaycay, J., Mumford, R. A., Swiderek, K. M., Lee, T. D., Ding, A., Troso, T., & Nathan, C. F. (1992) *Science 256*, 225−228.
6. Deng, W. D., Thiel, B. A., Tannenbaum, C. S., Hamilton, T. A., & Stuehr, D. J. (1993) *J. Immunol. 151*, 322−329.
7. Guo, F. H., De Raeve, H. R., Rice, T. T., Stuehr, D. J., Thunnissen, F. B. J. M., & Erzurum, S. C. (1995) *Proc. Natl. Acad. Sci. U.S.A. 92*, 7809−7813.
8. Kwon, N. S., Nathan, C. F., Gilker, C., Griffith, O. W., Matthews, D. E., & Stuehr, D. J. (1990) *J. Biol. Chem. 265*, 13442−13445.
9. Stuehr, D. J., Kwon, N. S., Nathan, C. F., Griffith, O. W., Feldman, P. L., & Wiseman, J. (1991) *J. Biol. Chem. 266*, 6259−6263.
10. Klatt, P., Schmidt, K., Uray, G., & Mayer, B. (1993) *J. Biol. Chem. 268*, 14781−14787.
11. Marletta, M. A. (1993) *J. Biol. Chem. 268*, 12231−12234.
12. Korth, H.-G., Sustmann, R., Thater, C., Butler, A. R., & Ingold, K. U. (1994) *J. Biol. Chem. 269*, 17776−17779.
13. Cho, H. J., Xie, Q.-W., Calaycay, J., Mumford, R. A., Swiderek, K. M., Lee, T. D., & Nathan, C. F. (1992) *J. Exp. Med. 176*, 599−604.
14. Sheta, E. A., McMillan, K., & Masters, B. S. S. (1994) *J. Biol. Chem. 269*, 15147−15153.
15. Ghosh, D. K., & Stuehr, D. J. (1995) *Biochemistry 34*, 801−807.
16. Chen, P.-F., Tsai, A.-L., Berka, V., & Wu, K. K. (1996) *J. Biol. Chem. 271*, 14631−14635.
17. Masters, B. S. S., McMillan, K., Sheta, E. A., Nishimura, J. S., Roman, L. J., & Martasek, P. (1996) *FASEB J. 10*, 552−559.
18. Chen, P.-F., Tsai, A.-L., & Wu, K. K. (1994) *J. Biol. Chem. 269*, 25062−25066.
19. McMillan, K., & Masters, B. S. S. (1995) *Biochemistry 34*, 3686−3693.
20. Richards, M. K., Clague, M. J., & Marletta, M. A. (1996) *Biochemistry 35*, 7772−7780.
21. Sari, M.-A., Booker, S., Jaouen, M., Vadon, S., Boucher, J.-L., Pompon, D., & Mansuy, D. (1996) *Biochemistry 35*, 7204−7213.
22. Xie, Q.-W., Leung, M., Fuortes, M., Sassa, S., & Nathan, C. (1996) *Proc. Natl. Acad. Sci. U.S.A. 93*, 4891−4896.
23. McMillan, K., & Masters, B. S. S. (1993) *Biochemistry 32*, 9875−9880.
24. Wang, J., Stuehr, D. J., Ikeda-Saito, M., & Rousseau, D. L. (1993) *J. Biol. Chem. 268*, 22255−22258.
25. Sono, M., Stuehr, D. J., Ikeda-Saito, M., & Dawson, J. H. (1995) *J. Biol. Chem. 270*, 19943−19948.
26. Salerno, J. C., Martasek, P., Roman, L. J., & Masters, B. S. S. (1996) *Biochemistry 35*, 7626−7630.
27. Abu-Soud, H. M., & Stuehr, D. J. (1993) *Proc. Natl. Acad. Sci. U.S.A. 90*, 10769−10772.
28. Abu-Soud, H. M., Gachhui, R., Raushel, F. M., & Stuehr, D. J. (1997) *J. Biol. Chem. 272*, 17349−17353.
29. Abu-Soud, H. M., Presta, A., Mayer, B., & Stuehr, D. J. (1997) *Biochemistry 36*, 10811−10816.
30. Kwon, N. S., Nathan, C. F., & Stuehr, D. J. (1989) *J. Biol. Chem. 264*, 20496−20501.
31. Tayeh, M. A., & Marletta, M. A. (1989) *J. Biol. Chem. 264*, 19654−19658.
32. Hevel, J. M., & Marletta, M. A. (1992) *Biochemistry 31*, 7160−7165.
33. Klatt, P., Schmid, M., Leopold, E., Schmidt, K., Werner, E. R., & Mayer, B. (1994) *J. Biol. Chem. 269*, 13861−13866.
34. Giovanelli, J., Campos, K. L., & Kaufman, S. (1991) *Proc. Natl. Acad. Sci. U.S.A. 88*, 7091−7095.
35. Baek, K. J., Thiel, B. A., Lucas, S., & Stuehr, D. J. (1993) *J. Biol. Chem. 268*, 21120−21129.
36. Klatt, P., Schmidt, K., Lehner, D., Glatter, O., Bachinger, H. P., & Mayer, B. (1995) *EMBO J. 14*, 3687−3695.
37. Wang, J., Stuehr, D. J., & Rousseau, D. L. (1995) *Biochemistry 34*, 7080−7087.
38. Mayer, B., Wu, C., Gorren, A. C. F., Pfeiffer, S., Schmidt, K., Clark, P., Stuehr, D. J., & Werner, E. R. (1997) *Biochemistry 36*, 8422−8427.
39. Tzeng, E., Billiar, T. R., Robbins, P. D., Loftus, M., & Stuehr, D. J. (1995) *Proc. Natl. Acad. Sci. U.S.A. 92*, 11771−11775.
40. Ghosh, D. K., Abu-Soud, H. M., & Stuehr, D. J. (1996) *Biochemistry 35*, 1444−1449.
41. Ghosh, D. K., Wu, C., Pitters, E., Moloney, M., Werner, E. R., Mayer, B., & Stuehr, D. J. (1997) *Biochemistry*, 36, 10609−10619.
42. Griscavage, J. M., Fukuto, J. M., Komori, Y., & Ignarro, L. J. (1994) *J. Biol. Chem. 269*, 21644−21649.
43. Mayer, B., Klatt, P., Werner, E. R., & Schmidt, K. (1995) *J. Biol. Chem. 270*, 655−659.
44. Mayer, B., John, M., Heinzel, B., Werner, E. R., Wachter, H., Schultz, G., & Bohme, E. (1991) *FEBS Lett. 288*, 187−191.
45. Kaufman, S. (1995) *Adv. Enzymol. Relat. Areas Mol. Biol. 70*, 103−220.
46. Kerwin, J. F., Jr., Lancaster, J. R., Jr., & Feldman, P. L. (1995) *J. Med. Chem. 38*, 4343−4362.
47. Witteveen, C. F. B., Giovanelli, J., & Kaufman, S. (1996) *J. Biol. Chem. 271*, 4143−4147.
48. Wu, C., Zhang, J., Abu-Soud, H., Ghosh, D. K., & Stuehr, D. J. (1996) *Biochem. Biophys. Res. Commun. 222*, 439−444.
49. Stuehr, D. J., & Ikeda-Saito, M. (1992) *J. Biol. Chem. 267*, 20547−20550.

50. Abu-Soud, H. M., Wang, J., Rousseau, D. L., Fukuto, J. M., Ignarro, L. J., & Stuehr, D. J. (1995) *J. Biol. Chem. 270*, 22997−23006.
51. Abu-Soud, H. M., Loftus, M., & Stuehr, D. J. (1995) *Biochemistry 34*, 11167−11175.
52. Siddhanta, U., Wu, C., Abu-Soud, H. M., Zhang, J., Ghosh, D. K., & Stuehr, D. J. (1996) *J. Biol. Chem. 271*, 7309−7312.
53. Feelisch, M., & Noack, E. A. (1987) *Eur. J. Pharmacol. 139*, 19−30.
54. Abu-Soud, H. M., Feldman, P. L., Clark, P., & Stuehr, D. J. (1994) *J. Biol. Chem. 269*, 32318−32326.
55. Sennequier, N., & Stuehr, D. J. (1996) *Biochemistry 35*, 5883−5892.
56. McMillan, K., Bredt, D. S., Hirsch, D. J., Snyder, S. H., Clark, J. E., & Masters, B. S. S. (1992) *Proc. Natl. Acad. Sci. U.S.A. 89*, 11141−11145.
57. Martinis, S. A., Blanke, S. R., Hager, L. P., Sligar, S. G., Hoa, G. H. B., Rux, J.J., & Dawson, J. H. (1996) *Biochemistry 35*, 14530−14536.
58. Matsuoka, A., Stuehr, D. J., Olson, J. S., Clark, P., & Ikeda-Saito, M. (1994) *J. Biol. Chem. 269*, 20335−20339.
59. Gerber, N. C., Rodriguez-Crespo, I., Nishida, C. R., & Ortiz de Montellano, P. R. (1997) *J. Biol. Chem. 272*, 6285−6290.
60. Sligar, S. G. (1976) *Biochemistry 15*, 5399−5406.
61. Fisher, M. T., & Sligar, S. G. (1985) *J. Am. Chem. Soc. 107*, 5018−5019.
62. Raag, R., & Poulos, T. L. (1989) *Biochemistry 28*, 917−922.
63. Gorren, A. C. F., List, B. M., Schrammel, A., Pitters, E., Hemmens, B., Werner, E. R., Schmidt, K., & Mayer, B. (1996) *Biochemistry 35*, 16735−16745.
64. Calaycay, J. R., Kelly, T. M., MacNaul, K. L., McCauley, E. D., Qi, H., Grant, S.K., Griffin, P. R., Klatt, T., Raju, S. M., Nussler, A. K., Shah, S., Weidner, J. R., Williams, H. R., Wolfe, G. C., Geller, D. A., Billiar, T. R., MacCoss, M., Mumford, R. A., Tocci, M. J., Schmidt, J. A., Wong, K. K., & Hutchinson, N. I. (1996) *J. Biol. Chem. 271*, 28212−28219.
65. Hurshman, A. R., & Marletta, M. A. (1995) *Biochemistry 34*, 5627−5634.
66. Werner, E. R., Pitters, E., Schmidt, K., Wachter, H., Werner-Felmayer, G., & Mayer, B. (1996) *Biochem. J. 320*, 193−196.

BI971944C